Pharm Res (2014) 31:768–779
DOI 10.1007/s11095-013-1198-x

RESEARCH PAPER

Complexation of Cell-Penetrating Peptide–Polymer Conjugates with Polyanions Controls Cells Uptake of HPMA Copolymers and Anti-tumor Activity

Yosi Shamay • Lina Shpirt • Gonen Ashkenasy • Ayelet David

Received: 11 June 2013 / Accepted: 21 August 2013 / Published online: 10 September 2013

ABSTRACT

Purpose Cell penetrating peptides (CPPs) can mediate effective delivery of their associated drugs and drug carriers intracellularly, however their lack of cell specificity remains a major obstacle for their clinical development. We aimed at improving the cell specificity and therapeutic efficacy of HPMA copolymer-octaarginine (R8) conjugate (P-R8) in cells at the tumor micro-environment.

Methods To avoid premature cell-penetration, the positively charged R8 moieties were masked via electrostatic complexation with various polyanionic molecules (heparin sulfate, hyaluronic acid, fucoidan and poly-glutamic acid). We followed the kinetics of the FITC-labeled P-R8 penetration into endothelial and cancer cells over-time after its complexation *in vitro* and further tested whether the *in situ* addition of a stronger polycation can trigger the release of P-R8 from the complexes to resume cell penetration activity. A murine model of B16-F10 lung metastasis was then used as an *in vivo* model for assessing the therapeutic efficacy of the P-R8, loaded with doxorubicin (P-R8-DOX), after its complexation with PGA.

Results The intracellular penetration of P-R8-FITC was reversibly inhibited by forming electrostatic interactions with counter polyanions, and can be restored either gradually over time by dissociation from the polyanions, or promptly following the addition of protamine sulfate. Mice injected with B16-F10 cells and treated with P-R8-DOX/PGA complexes, exhibited a significant prolonged survival times when compared with DOX-treated mice or relative to mice treated with either P-R8-DOX or P-DOX alone.

Conclusions The gradual release of P-R8 from P-R8-DOX/PGA may improve the therapeutic efficacy of water-soluble based nanomedicines for the treatment of solid lung tumors.

KEY WORDS cell penetrating peptides · drug delivery · HPMA copolymer · polymeric complexes

ABBREVIATIONS

AIBN	2,2'-azobis(isobutyronitrile)
CPPs	Cell-penetrating peptides
DOX	Doxorubicin
EPR	Enhanced permeability and retention
Fi	Fucoidan
FITC	Fluorescein-5-isothiocyanate
HA	Hyaluronic acid
Hep	Heparin
HMW-Hep	High molecular weight heparin
HPMA	N-(2-hydroxypropyl)methacrylamide
LMW-Hep	Low molecular weight heparin
MTT	3-(4,5-dimethylthiazol-2-yl)-2,5-diphenyltetrazolinium bromide
PFA	Paraformaldehyde
PGA	Poly-(l)-glutamic acid
PMA	Poly(methacrylic acid)
R8	Octaarginine
SEC	Size-exclusion chromatography

INTRODUCTION

Current chemotherapeutic treatments used for treating cancer are limited by difficulties in delivering anticancer drugs to the tumor micro-environment at therapeutic concentrations.

Y. Shamay • L. Shpirt • A. David
Department of Pharmacology, Faculty of Health Sciences
Ilse Katz Institute for Nanoscale Science and Technology
Ben-Gurion University of the Negev, Beer-Sheva 84105, Israel

G. Ashkenasy
Department of Chemistry, Faculty of Natural Sciences
Ilse Katz Institute for Nanoscale Science and Technology
Ben-Gurion University of the Negev, Beer-Sheva 84105, Israel

A. David (✉)
Department of Pharmacology, Faculty of Health Sciences
Ben-Gurion University of the Negev, Beer-Sheva 84105, Israel
e-mail: ayeletda@bgu.ac.il

Most anti-cancer agents are low molecular weight (LMW) hydrophobic molecules and, therefore, exhibit poor pharmacokinetics and limited bio-distribution profiles. Consequently, only small amounts of drug succeed in reaching the tumor site, and therapy is associated with severe and harmful toxic effects on normal organs and tissues. Several passively and actively targeted drug delivery systems, including, liposomes, polymer conjugates, polymeric micelles, nanoparticles, dendrimers and antibodies have been utilized over the years in attempts to overcome this limitation by increasing drug concentrations at the affected areas while decreasing accumulation at non-target organs (1–6). These nano-sized carriers can accumulate passively at the tumors site, owing to the discontinuous endothelium of angiogenic tumor vasculature and the lack of effective tumor lymphatic drainage, a mechanism known as the 'enhanced permeability and retention' (EPR) effect (7,8). Still, the physiological properties of tumors, i.e., cellular packing, high interstitial fluid pressure in the tumor core and dense extracellular matrix, limit the diffusion of many small-molecule drugs and macromolecules within tumor tissue (9–11). Despite the fact that many actively targeted delivery systems have been designed by several groups (12–14), including the authors' (15–20), to improve the transport of the associated drug carriers into a targeted cell (such as via receptor-mediated endocytosis), the primary drawback in the use of an active targeting strategy is the low degree or heterogeneity of receptor expression in different tumor cells.

Cell-penetrating peptides (CPPs) are short cationic, often arginine-rich, amino acid sequences that promote receptor-independent intracellular delivery of a broad variety of cargo, including nanoparticulate pharmaceutical carriers (21,22). However, the lack of cell specificity remains a major obstacle limiting the clinical development of CPPs-based therapeutics. Thus, several strategies, largely based on reversible shielding of the CPP sequence by steric hindrance, and de-shielding in the tumor micro-environment by exploiting the peritumoral pH (23,24) or enzymatic activity (25,26), have been developed to avoid non-specific uptake into non-target organs and tissues. Since large inter-individual variability in enzymatic activity or in intra-tumoral pH exists, we sought alternative approaches for activating CPP function independent of extracellular features of the tumor micro-environment. Accordingly, we recently described a light-activated approach to 'switch on' the activity of a CPP attached to *N*-(2-hydroxypropyl)methacrylamide (HPMA) copolymer-$_D$(KLAKLAK)$_2$ conjugates, so as to promote intracellular drug penetration and cytotoxicity in different cancer cell types (27). However, the wavelength at which the photo-cleavable caging component of the molecule can be removed (365 nm) limits the application of our system to areas of the body that can only be illuminated directly. In the following, we now report that the intracellular penetration of HPMA copolymer conjugates bearing dye or drug moieties and the CPP octaarginine (P-R8) can be reversibly inhibited by forming electrostatic interactions with polyanionic molecules. Interestingly, we observed that depending on the type of polyanionic molecule we selected or the working conditions, cell penetration can be restored over time or promptly following the addition of a stronger polycation (Scheme 1). The gradual dissociation of the CPP moieties from the polyanions over time was further studied as a tool to improve anti-cancer activity *in vivo*.

HPMA copolymer is water-soluble, biocompatible, non-immunogenic and non-toxic, and enables selective delivery of drugs into tumor tissues (28). However, since HPMA possesses a non-degradable polymeric backbone, the renal threshold limits the applicable MW to well below 40 kDa. This in turn may lower the retention time of the conjugate in circulation, and thereby decreasing its passive accumulation at the tumor site with a concomitant decrease in pharmaceutical efficiency (2). An additional advantage in complexation of the P-R8 conjugates to high MW biodegradable polyanions would thus be an increase in size of the drug carrier, together with improved passive accumulation in tumors, while avoiding penetration into non-target organs.

In this study, we have followed the kinetics of P-R8-FITC penetration into endothelial and cancer cells over time, after complexation of the compound with negatively charged polysaccharides and polypeptides. We further tested whether the *in situ* addition of a counter polycation can trigger the release of P-R8-FITC from complexes, leading to resumption of cell penetration activity. The most suitable conjugates bearing the cytotoxic drug doxorubicin (DOX) were then tested *in vivo* for anti-cancer activity in a murine B16-F10 lung metastasis model.

MATERIALS AND METHODS

Materials

All chemicals were of reagent grade and were obtained from Sigma–Aldrich (Rehovot, Israel), unless otherwise stated. p-nitrophenol, tert-butyl carbazate and o-phenylenediamine were purchased from Acros Organics. Fmoc-protected amino acids, the peptide coupling reagent 2-(1H-Benzotriazole-1-yl)-1,1,3,3-tetramethylaminium hexafluorophosphate (HBTU), and resins were purchased from Novabiochem-Merck (Darmstdt, Germany). 3-aminopropyl methacryl amide was purchased from Polysciences (UK), Hyaluronic acid 12 kDa from Lifecore (US). B16-F10 malignant mouse melanocytes and bEnd.3 mouse brain microvascular endothelial cells were purchased from ATCC (Manassas, VA). The cells were grown in DMEM culture medium supplemented with 10% fetal calf serum, and 2 mM glutamine (100 U/ml) and penicillin/

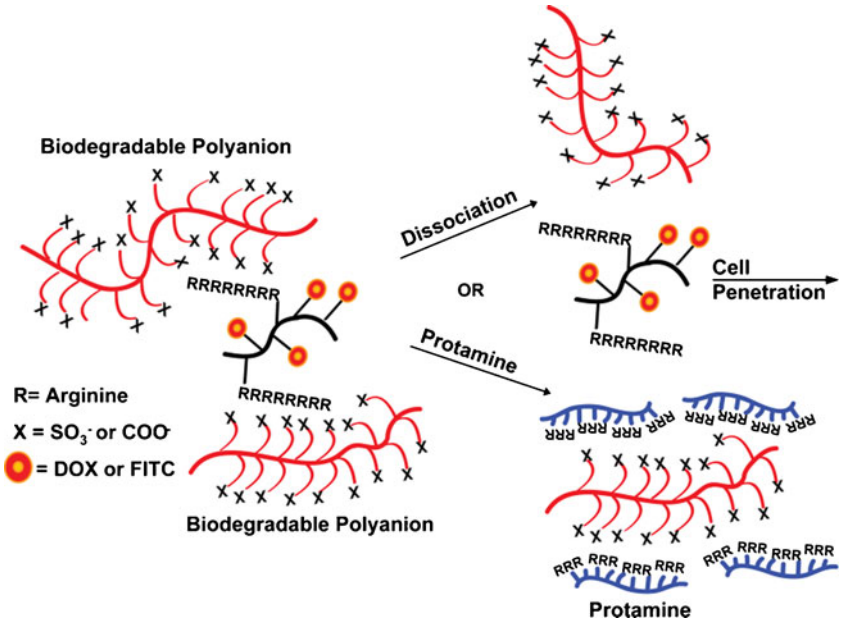

Scheme 1 HPMA copolymer-octa-arginine conjugate (P-R8) can penetrate cells only after gradual dissociation from the biodegradable polyanions over time, or following the addition of a stronger counter polycation molecule (protamine).

streptomycin (100 mg/ml). All ingredients were purchased from Biological Industries, Kibbutz Beit-Haemek, Israel. C57BL/6 mice were obtained from Harlan Laboratories (Rehovot, Israel) Mice were used at 8–10 weeks of age, housed in accordance with approved institutional guidelines. All experiments were approved by the Ben-Gurion University of the Negev Care and Use Animal Committee.

Synthesis of Monomers and K-R8 Peptide

NH_2-KRRRRRRRR-$CONH_2$ (K-R8) was synthesized on solid-phase Rink-Amide MBHA resin at 0.1 mmol scale using the Fmoc-based chemistry. Peptide synthesis grade solvents (DMF and CH_2Cl_2), HBTU and *N*,*N*-Diisopropylethylamine (DIPEA) were used for all syntheses. The peptide was purified by semi-preparative HPLC (Thermo-Finnegan), and identity and purity were analyzed by analytical HPLC (Dionex), and LCMS (Thermo): M+1393. The monomers HPMA (29), methacryloyl-glycylglycine p-nitrophenyl ester (MA-GG-ONp) (30), methacryloyl-aminopropyl fluorescein-5-isothiocyanate (MAP–FITC) (31) and MA-GG-HZBoc (32) were synthesized as described previously.

Synthesis of HPMA Copolymer Precursors

The FITC-labeled HPMA copolymer precursor having active ester groups for peptide attachment (designated as P-(GG-ONp)-FITC, where P represents the HPMA copolymer backbone) was synthesized by random radical precipitation copolymerization in a sealed vial in acetone/DMSO mixture at 50°C for 24 h using AIBN as the initiator. The feed molar percentage of the monomers was 88:10:2 for HPMA, MA-GG-ONp and MAP–FITC, respectively. The ratio of monomers to initiator and solvent was 12.5:0.6:86.9 wt%, respectively. The copolymer precursor with active ester groups and protected hydrazone bonds (P-(GG-ONp)-HZBoc), which later used for peptide and DOX attachment respectively, was synthesized by copolymerizing HPMA, MA-GG-ONp and MA-GG-HZBoc at 82:10:8 mol%, respectively, as described above. After 24 h the solvent was evaporated, and the polymers dissolved in methanol and precipitated in cold acetone:ether mixture (1:2). The copolymers were isolated, purified and fractionated by size-exclusion chromatography (SEC) on AKTA- fast protein liquid chromatography (FPLC) system (Amersham Pharmacia Biotech) equipped with UV and RI (Shodex) detectors, using Sephadex LH-20 column with methanol as eluent. The copolymer fractions were collected, concentrated, precipitated in diethyl ether and dried in a desiccator overnight. P-(GG-ONp)-FITC and P-(GG-ONp)-HZBoc were attained at 58% and 63% yield, respectively. The number of ONp groups in both P-(GG-ONp)-FITC and P-(GG-ONp)-HZBoc precursor copolymers was estimated by following the UV absorption (400 nm) during the release of *p*-nitrophenol from the copolymers in 1 N sodium hydroxide solution. FITC loading was determined from its UV absorbance at 492 nm. The amount of MA-GG-HZBoc moieties was assessed by ^{1}H NMR in D_2O, using the Boc *t*-butyl protons chemical shift (δ 1.40, s, 9H) for the calculation. The weight average molecular weight (M_w) and polydispersity (I) of the copolymers were determined by SEC, using Sephacryl 16/60 S-400 column (GE Healthcare) with PBS buffer pH 7.4, calibrated with fractions of known molecular weight HPMA copolymers. The

characteristics of the polymers and the methods used for characterization are summarized in Table I.

Synthesis of the FITC-Labeled HPMA Copolymer Octaarginine Conjugate; P-R8-FITC

The N-terminal lysine harboring octaargigine (K-R8) was coupled to P-(GG-ONp)–FITC via aminolysis. Briefly, the polymer precursor P-(GG–ONp)-FITC (60 mg) was dissolved in anhydrous DMSO (1 mL) containing triethyl amine (80 μL). K-R8 (8 mg, ~12 mol% relative to ONp groups), was then added to the solution and mixed for 24 h. The unreacted ONp ester groups were hydrolyzed by dilution in 1.5 ml DDW at pH 9 for 2 h. The reaction mixture was purified twice on a Sephadex G-25 (PD-10) column and lyophilized to give P–R8–FITC at 77% yield. The Mw of P–R8–FITC was estimated by SEC on AKTA FPLC system, using Sephacryl S-400 column, calibrated with fractions of known molecular weight HPMA copolymers (Table I). The content of conjugated peptide was estimated from ^{1}H-NMR (Table I) protons chemical shift of R8 (δ 1.7, s, 16H). A control polymer without K-R8 (P-FITC) was obtained by hydrolyzing the ONp groups from P-(GG-ONp)-FITC in 1 N sodium hydroxide solution, followed by purification on a PD-10 column.

Synthesis and Characterization of DOX-Containing HPMA copolymer-R8 Conjugate; P-R8-DOX

The DOX containing HPMA copolymer–R8 conjugate was prepared by a three-step procedure. K-R8 was first attached to the active ester linker of (P-(GG-ONp)-HZBoc) by aminolysis, as described above. The Boc protecting groups were removed by concentrated TFA, and DOX was attached to the free hydrazone groups in methanol at the presence of catalytic amount of acetic acid, as described (32) to give P-R8-DOX in 43% yield. The control DOX-containing copolymer without K-R8, P-DOX was prepared by attaching DOX to P-(GG-ONp)–HZBoc precursor, from which the ONp groups were first released in 1 N sodium hydroxide solution. The conjugates were isolated and purified on LH-20 column using methanol as eluent. Copolymer conjugates were characterized by SEC on FPLC system, using Sephacryl S-400 column. The total DOX content was determined by UV spectrophotometry ($\lambda = 488$ nm, $\varepsilon = 11{,}500$ L mol^{-1} cm^{-1}, water).

Table I Characteristics of HPMA Copolymer-R8 Conjugates Bearing FITC or DOX and Their Control Polymers Lacking the R8 Peptide

HPMA Conjugate	MW (kDa)[a]	I	% mol FITC[b]	% mol DOX	% mol R8 peptide[c]	Number of Arg per macromolecule[d]
P-R8-FITC	19.1	1.6	1.8	–	2.5	24
P- FITC	18.3	1.6	1.8	–	–	–
P-R8-DOX	18	1.5	–	8.2	1.8	20
P-DOX	17.2	1.5	–	7.5	–	–

[a] Estimated by size exclusion chromatography (SEC) on AKTA FPLC system, using Sephacryl S-400 column (GE healthcare), calibrated with fractions of known molecular weight HPMA copolymers

[b] Determined spectroscopically by UV absorbance at 492 nm

[c] Estimated from ^{1} H-NMR

[d] Calculated from the wt% of the peptide content

Preparation and Characterization of Polymeric Complexes

P-R8-FITC (2 mg/ml) and of polyanions (2 mg/ml) were complexed at 1:3 molar ratio, respectively, in 0.15 M NaCl solution. The mixtures were vortexed for 3 seconds and kept still at room temperature for 10 min. The size of the complexes was characterized by dynamic light scattering (DLS) BI 2030AT (Brookhaven Instruments) at a scattering angle of 90° at room temperature.

In Vitro Release of DOX from P-R8-DOX/polyanion Complexes

The rate of DOX release from P-R8-DOX/polyanion complexes was investigated by incubating the conjugate in PBS at pH 5.5 or 7.4 at 37°C. The concentration of the P-R8-DOX in solution was equivalent to 1 μM DOX. The amount of released DOX was determined by extracting free DOX into chloroform and measuring absorbance at 492 nm. All drug-release data are expressed as the amounts of free drug relative to the total drug content in the conjugates. All experiments were carried out in duplicates.

Cell Penetration Activity of P-R8-FITC Following its Complexation with Different Polyanionic Molecules

P-R8-FITC and the polyanions were complexed, as described above, and kept still at room temperature for 10 min before dilution with DMEM growth medium to a final concentration of 50 μg/ml P-R8-FITC. bEND.3 cell monolayers were grown in a 24 wells plate for 24 h, and then incubated with P-R8-FITC/polyanion complexes for another 1 h, washed twice with hanks balanced solution, trypsinized, collected, rinsed with cold PBS and the cell-associated fluorescence was determined immediately using flow cytometry system (GUAVA Mini Easycyte) excitation at 485 nm, emission at 525 nm.

Durability of Complexes Formed by P-R8-FITC and the Different Polyanions over Time

bEND.3 cell monolayers were incubated with P-R8-FITC (50 μg/ml) or P-R8-FITC/polyanions complexes in DMEM

growth medium for 24 h. For negative control a polymer that lacks the R8 peptide, P-FITC was used. At different time points cells were collected and the cell-associated fluorescence was determined immediately by flow cytometry, as described above. The % of P-R8-FITC activity of was calculated by the equation $\frac{F_{P-R8-FITC+polyanion} - F_{P-FITC}}{F_{P-R8-FITC} - F_{P-FITC}} \times 100\%$, where F = mean fluorescence value. The value of the negative control P-FITC was subtracted from all fluorescence values in order to eliminate the contribution of non-specific endocytosis. Experiments were done in triplicates.

Visualization of Cell Penetration at Different Incubation Times

B16-F10 or bEND.3 cells (3×10^4) were seeded onto cover slips in 24-well plates with 500 μL DMEM growth medium. 24 h after seeding, 50 μg/ml P-R8-FITC or P-R8-FITC/polyanion complexes containing 50 μg/ml P-R8-FITC were incubated for 24 h. At different time points cells were washed twice with hanks balanced solution fixed in 3% paraformaldehyde, stained with DAPI and mounted in Mowiol-DABCO mounting medium. Images were acquired with an Olympus FV1000-IX81 Confocal Microscope (exCitation at 488 nm, emission collected with a 515 nm barrier filter). Auto-fluorescence background was ascertained using control untreated cells.

Reversing the Polyanion-Induced Inhibition of P-R8-FITC by Protamine

To test whether protamine could be used to resume P-R8-mediated cell penetration, bEND.3 cell monolayers were incubated with 80 μg P-R8-FITC or P-R8-FITC/polyanion complexes (1:3) in DMEM growth medium. After 10 min 80 μg Protamine (in 0.4 ml) was added while slightly shaking the plate. The cells were then incubated for another 2 h, and the % of P-R8-FITC activity of was estimated by flow cytometry, as described above.

Visualization of Protamine Triggered Cell Penetration

bEND.3 cells (3×10^4) were seeded onto cover slips in 24-well plates with 500 μL DMEM growth medium and then incubated with P-R8-FITC or P-R8-FITC/polyanion complexes for another 2 h, with or without protamine, as described above. The cells were then washed, fixed in 3% paraformaldehyde, stained with DAPI and mounted in Mowiol-DABCO and visualized using a confocal microscope, as described above.

Murine B16-F10 Pulmonary Metastasis Model

WT C57BL/6 mice were injected via the tail vein with 1×10^6 B16-F10 cells on day 0. On day 7 after tumor cells inoculation, the mice were randomly divided into five groups of five mice, and treated by a single intravenous injection of free DOX at its maximum tolerated dose (6 mg/kg), P-DOX, P-R8-DOX and P-R8-DOX/PGA (1:3) at dose of 15 mg/kg DOX equivalent or PBS and then monitored for their survival (Kaplan-Meier method). 15 mg/kg DOX equivalent dose of HPMA copolymer-bound DOX has been previously reported to be well tolerated in mice, resulted in no measurable weight loss or other signs of toxicity (33).

RESULTS AND DISCUSSION

Synthesis and Characterization of P-R8/polyanion Complexes

Two types of HPMA copolymers bearing the R8 sequence were prepared (Fig. 1a and b). A FITC-labeled copolymer P-R8-FITC was prepared for tracking binding and intracellular fate *in vitro*, while a doxorubicin (DOX)-containing copolymer, P-R8-DOX, was employed for evaluating *in vivo* anti-cancer activity. The DOX molecules were attached to the polymer backbone via a pH-sensitive hydrazone group for facile release in lysosomal compartments. A detailed synthesis of the new polymers can be found in the Materials and Methods section, with characterization of the different compounds (MW, I, and Arg, FITC and DOX loading) being provided in Table I.

Complexes were formed by mixing P-R8 solution with a three-fold molar excess of the well-characterized polyanions (Fig. 2 and Table II) for 10 min at room temperature. As is evident from DLS measurements, P-R8-FITC and P-R8-DOX form complexes with diameters of ~80–140 nm with all polyanions, apart from 4.5 kDa Heparin, for which smaller complexes (10 nm) were obtained (Fig. 3). P-R8-DOX complexes were found to be slightly larger than were P-R8-FITC complexes, most probably due to the high content of DOX in the HPMA copolymer backbone (8 mol%), a factor that may induce hydrophobic interactions. All complexes had a mildly negative zeta potential of -6.3 ± 0.7 mV due to an excess of negatively charged groups of the polyanion.

DOX Release from P-R8-DOX/polyanion Complexes at Physiological and Acidic pH

We have next evaluated the *in vitro* stability of P-R8-DOX complexes formed with different polyanions at physiological and acidic pH conditions. Figure 4a indicates that only P-R8-DOX/PGA complexes demonstrated significant stability at physiological pH. The early release of DOX from the sulfated polysaccharide might be attributed to the local acidic pH inside the complexes which could catalyze the hydrolysis of the pH-sensitive hydrazone bond. Incubation of P-R8-DOX/

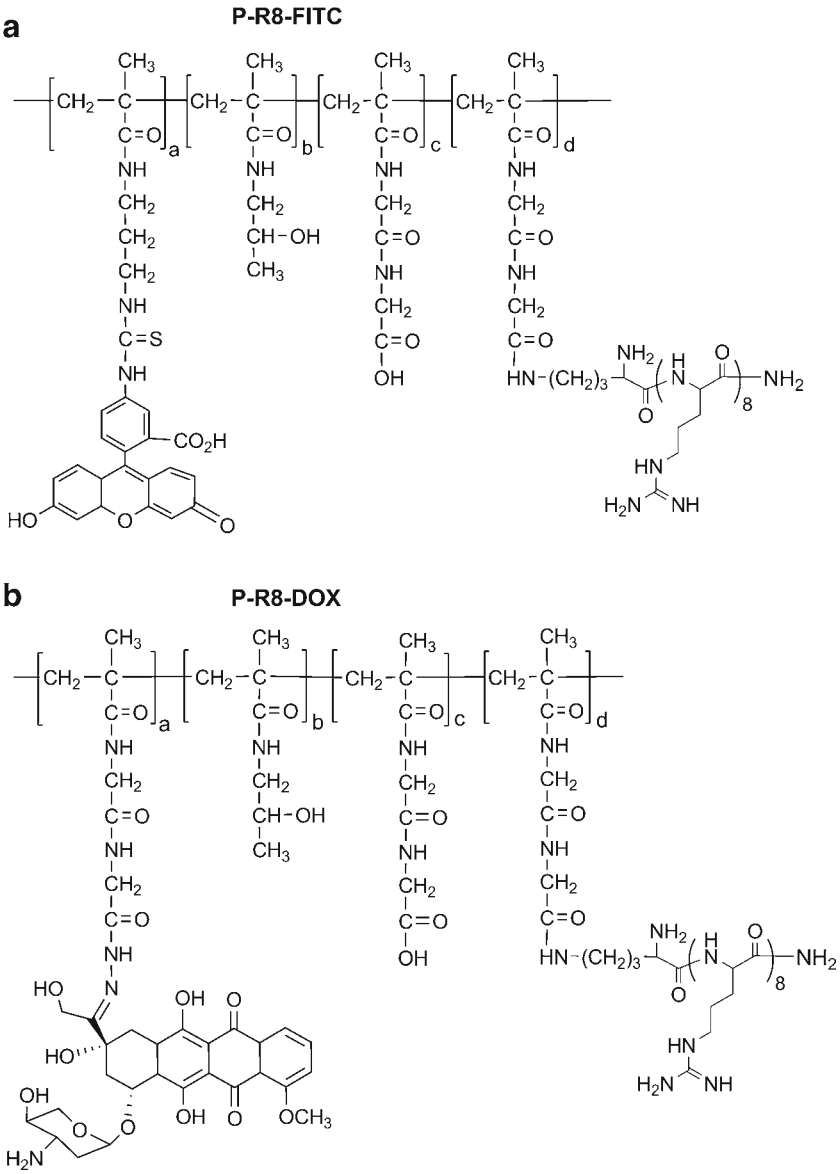

Fig. 1 Structure of the FITC-labeled HPMA copolymer conjugate P-R8-FITC (**a**), and Doxorbicin-containing HPMA copolymer conjugate, in which DOX moieties are attached via a pH sensitive hydrazone bond, P-R8-DOX (**b**).

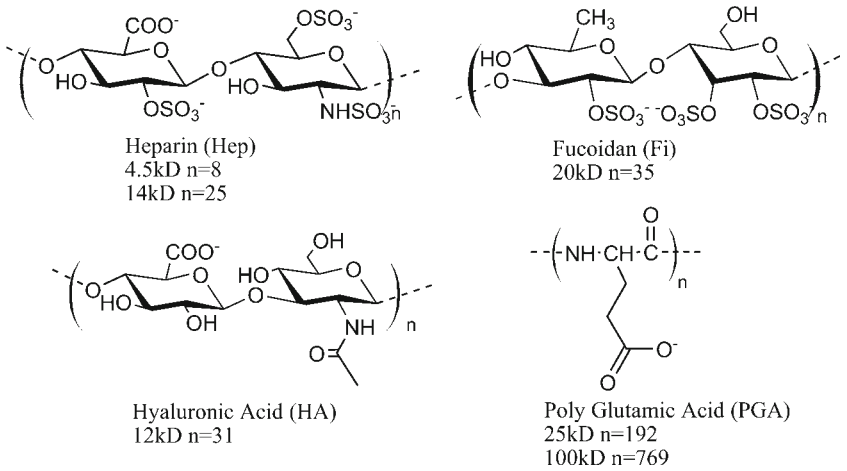

Fig. 2 Structures of various polyanions used for electrostatic complexation.

Table II Characteristics of the Different Biodegradable Polyanions Tested for Complexation with HPMA copolymer-R8 conjugates

Biodegradable Polyanion	Mw (kD)	Number of COO^- per macromolecule	Number of SO_3^- per macromolecule	Abbreviation
Fucoidan	20	–	60	Fi 20 kDa
Heparin	14	25	75	Hep 14 kDa
LMW Heparin	4.5	8	24	Hep 4.5 kDa
Poly (l) Glutamic acid	25	192	–	PGA 25 kDa
Poly (l) Glutamic acid	100	769	–	PGA 100 kDa
Hyaluronic acid	12	31	–	HA 12 kDa

polyanion complexes in mildly acidic conditions (pH ~5.5), modeling the endosomal and lysosomal environment, resulted in an increased rate of DOX release from complexes (Fig. 4b). In cases where sulfated polysaccharides are desired for complexation with R-R8, peptide linkers, such as the cathepsin B-cleavable GFLG sequence[2], would be more suitable for mediating drug attachment.

Cell-Penetrating Activity of P-R8-FITC Following Complexation with Different Polyanions

Control over the cell-penetration activity of P-R8-FITC resulting from electrostatic interactions with the different polyanions was estimated by flow cytometry after 1 h of incubation with murine endothelial bEND.3 cells (Fig. 5a and b). The complexation of P-R8-FITC with all studied polyanions, except HA, strongly inhibited cell penetration. The multiple sulfate groups of Hep and Fi (Fig. 5a) or the carboxyl groups of PGA (Fig. 5b) interacted with the guanidinium groups on R8 to neutralize cationic residues, thereby diminishing the ability of R8 to interact with bEND.3 cell membranes and mediate cell penetration. Although the carboxylated polysaccharide HA can form stable complexes with P-R8-FITC (Fig. 3), it failed to inhibit cell penetration. The relatively low charge density of HA, and the fact that each of its 31 carboxylic acids are separated by neutral N-acetylglucosamines, might explain this result.

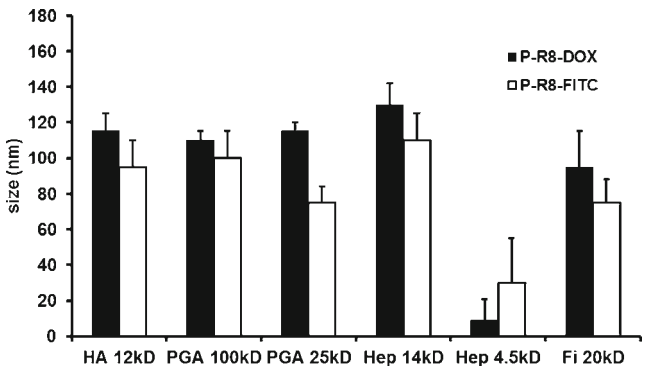

Fig. 3 Size of electrostatic complexes of P-R8-DOX and P-R8-FITC with various biodegradable polyanions as determined by DLS.

Cell Penetration Activity of P-R8-FITC/polyanion Complexes Over Time

The durability of complexes formed by P-R8-FITC with the different polyanions, when incubated with bEND.3 cells was further studied (Fig. 5c and d). Cells were incubated with P-R8-FITC/polyanion complexes for different time periods and cell-associated fluorescence was determined by flow cytometry. Sulfated polysaccharides (low and high Mw Hep, and Fi) formed stable complexes with P-R8-FITC and thus 'switched off' the cell penetrating activity of the compound for at least 24 h. On the other hand, complexation with carboxylated polyanions (low and high Mw PGA) was reversible, such that 80% of the cell-penetrating activity was recovered within 24 h post-treatment (Fig. 5c).

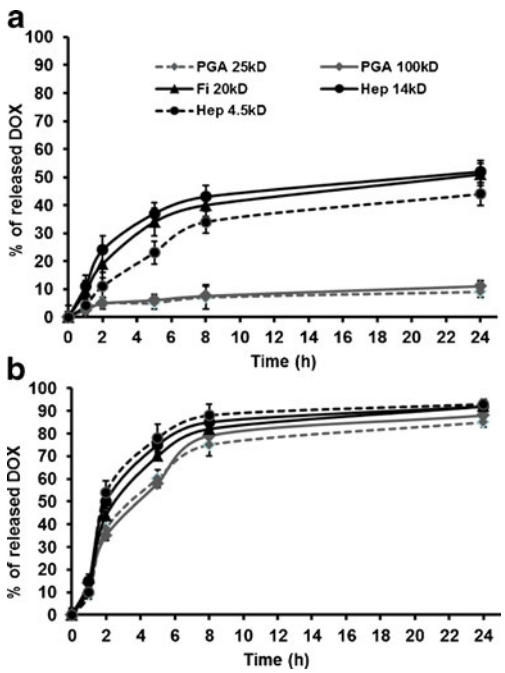

Fig. 4 Release of DOX from P-R8-DOX complexed with different polyanions at PBS pH 7.4 (**a**) and PBS pH 5.5 (**b**) at 37°C.

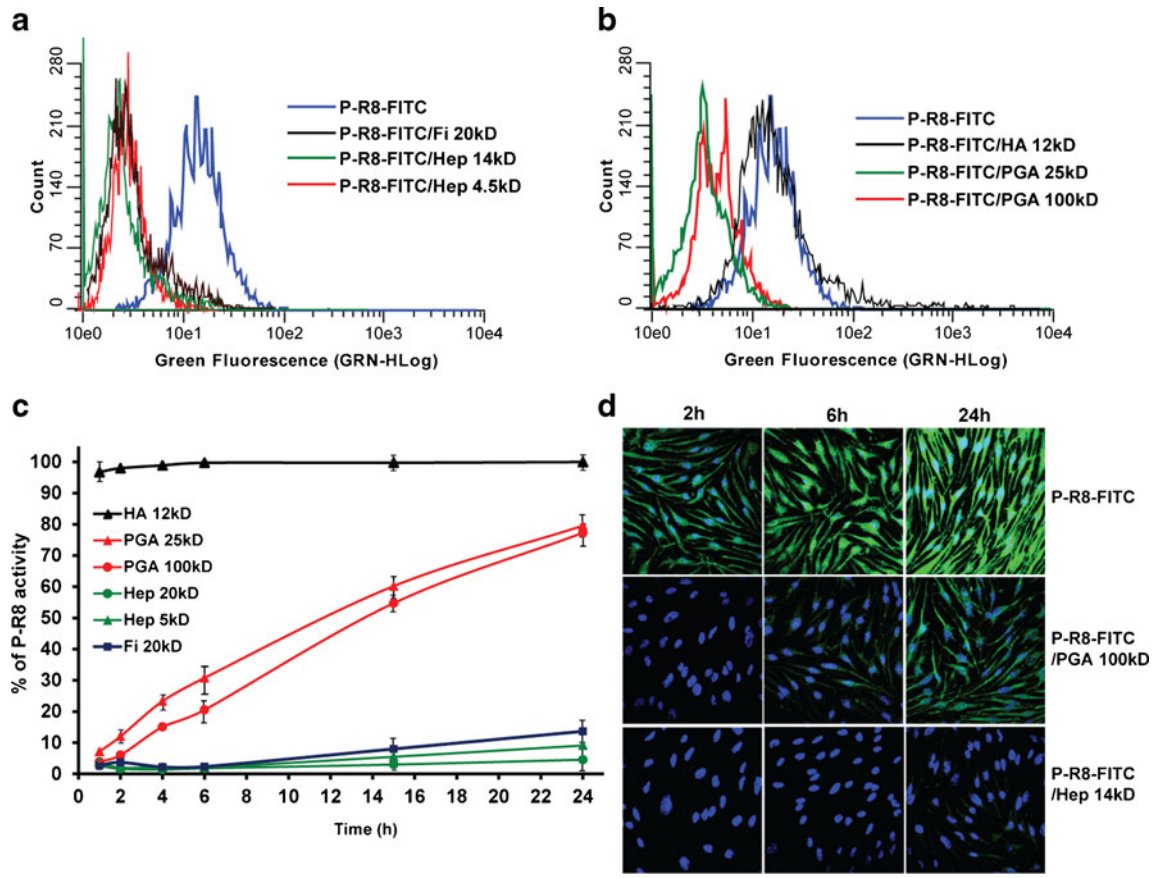

Fig. 5 Cell penetration activity of P-R8-FITC (50 μg/ml) following its complexation with sulfated (**a**) and carboxylated (**b**) polyanions, as determined by flow cytometry after 1 h of incubation with bEND.3 cells. (**c**) Cell penetration activity of P-R8-FITC over time, after its complexation with different polyanions in bEND.3 cells. The % of P-R8-FITC activity for the different complexes was calculated from mean fluorescence values obtained by flow cytometry. (**d**) Representative confocal images of bEND.3 cells incubated with P-R8-FITC/polyanion complexes at different time points.

Confocal microscopy further confirmed this observation in both endothelial (bEND.3, Fig. 5d) and cancer (B16-F10) cells (data not shown).

We proposed three different hypotheses to explain the driving force for reversible behavior of P-R8-FITC/PGA complexes. In the first, spontaneous dissociation of PGA from P-R8-FITC occurs, owing to its rigid backbone structure. Alternatively, weak binding affinity exists between the acidic residues of PGA and R8 residues. Finally, degradation of PGA by extracellular proteases secreted by cells may occur. To test these hypotheses, a non-degradable acidic polyanion, poly(methacrylic acid) (PMA; 20 kDa), and a cathepsin B non-cleavable D-PGA (made from all poly-D-glutamic acid; 100 kDa) were tested for their ability to block P-R8-FITC penetration. Complexation with PMA inhibited P-R8-FITC penetration over 24 h (Fig. 6) in the same manner as did the sulfated polysaccharide Fi. On the other hand, D-PGA interacted reversibly with P-R8-FITC, similarly to L-PGA, indicating that no extra-cellular cleavage had occurred. We thus suggest that the rigid peptidic backbone of PGA circumvents the formation of right conformations required for strong electrostatic interactions between the PGA and P-R8. In the presence of cancer or endothelial cells, cell-surface associated anionic phospholipids and glycosaminoglycans would compete with the carboxyl groups of PGA for binding to R8, thereby releasing P-R8-FITC which would carry its cargo into the cell.

Protamine-Induced Cell Penetration

The *in situ* addition of protamine sulfate, a 33 amino acids highly basic polypeptide, triggered the release of P-R8-FITC from complexes with sulfated and carboxylated polyanions and induced rapid cell penetration (Fig. 7). Protamine was added to cells that were pre-incubated (10 min) with P-R8-FITC/polyanion complexes at a sub toxic concentration (50 μg/ml), and we found that 60–97% of the cell penetrating activity of P-R8-FITC was recovered (Fig. 7a). Since protamine possesses strong affinity to sulfated polysaccharides (34) and PGA, it triggered the release of P-R8-FITC and its activity was restored, as confirmed by confocal microscopy

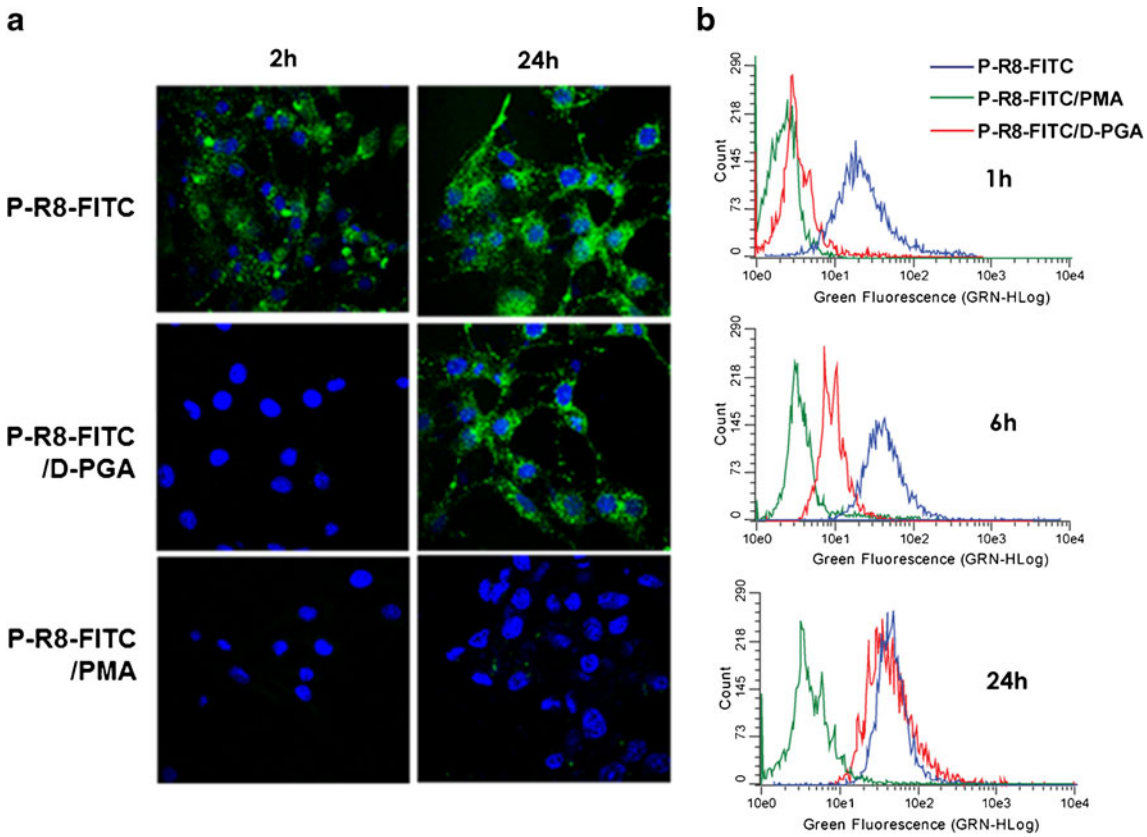

Fig. 6 (**a**) Representative confocal images of bEND.3 cells treated with P-R8-FITC and P-R8-FITC/non-degradable polyanion complexes, after 2 h and 24 h of incubated. The *green color* indicates P-R8-FITC associated fluorescence and the *blue color* shows nuclear DNA staining. (**b**) Cell penetration activity of P-R8-FITC and P-R8-FITC/non-degradable polyanion complexes into bEND.3 cells at different time points. The cell-associated fluorescence was measured by flow cytometry at 1, 6 and 24 h post treatment.

(Fig. 7b). Interestingly, the release of heparin from P-R8-FITC/Hep complexes depended on the heparin charge density. A full recovery of P-R8-FITC cell-penetrating activity was observed when protamine was added to the P-R8-FITC/LMW-Hep complexes, whereas only 70% of such activity was regained from the P-R8-FITC/HMW-Hep complexes. This observation can be explained by the fact that protamine, at sub toxic concentrations, binds the free, non-neutralized sulfate groups of the HMW-Hep in P-R8-FITC/complexes, yet does not efficiently interfere with the interactions of P-R8-FITC.

Complexation of P-R8 with the biodegradable PGA offer several potential advantages for selective drug delivery into cancerous tissues, namely improved tumor accumulation, owing to the increased size relative to P-R8, enhanced potency, given that such complexes can penetrate and eliminate both endothelial and cancer cells in the tumor micro-environment, independent of the tumor type or dedifferentiation, as well as higher selectivity by avoiding non-specific uptake into non-target organ and tissues while improving tissue penetration in the tumor microenvironment owing to the gradual and controlled release of P-R8 over time. The increased stability of P-R8/PGA complexes at physiological pH conditions is also desirable, as is the fact that P-R8/PGA complexes do not require the addition of a counter polycation to trigger drug release and cell penetration. For these reasons, we selected P-R8/PGA complexes for further *in vivo* study.

Anti-tumor Activity in a B16-F10 Pulmonary Metastasis Model

The anti-cancer effects of P-DOX, P-R8-DOX and P-R8-DOX/PGA complexes were evaluated in the B16-F10 pulmonary metastasis model. In these experiments, conducted 7 days after inoculation of B16-F10 cells, mice were randomly divided into five treatment groups and administered (i.v.) with a single dose of free DOX, polymers or polymer/PGA complexes, or with saline as a control. The total DOX dosage for all conjugates was 15 mg/kg. The P-R8-DOX/PGA treatment significantly prolonged experimental mice survival times up to 194%

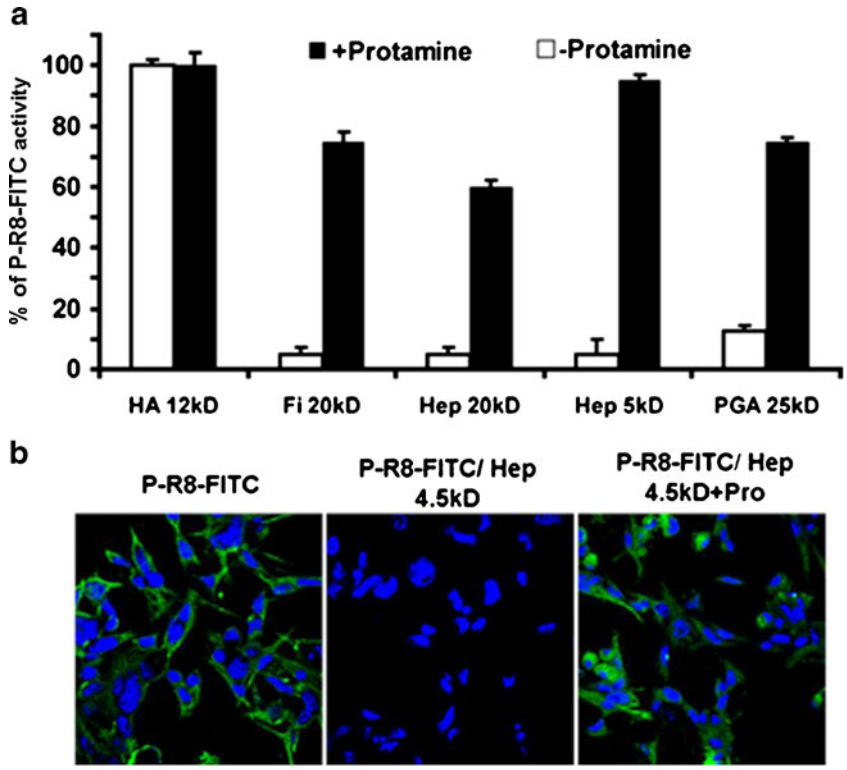

Fig. 7 (**a**) Cell penetration activity of P-R8-FITC (50 μg/ml), after its complexation with different polyanions, and further incubation with bEND.3 cells for 2 h, with or without protamine, as determined by flow cytometry. (**b**) Representative confocal images of bEND.3 cells treated with P-R8-FITC/Hep 4.5 kD complexes with or without protamine. The *green color* indicates P-R8-FITC associated fluorescence. DAPI was utilized for nuclear staining.

and 171%, relative to the survival rates achieved with the P-DOX and P-R8-DOX conjugates, respectively (Fig. 8), and when compared to free DOX. Most strikingly, 40% of mice (2 of 5) survived up to day 60 (when the experiment was terminated) with no measurable weight loss or other signs of toxicity. This suggests that a higher dose of P-R8-DOX/PGA complexes could potentially be used to attain greater therapeutic efficacy. P-R8-DOX alone was found to be only slightly better in prolonging mice survival than was P-DOX. The fact that just a single i.v. injection of P-R8-DOX/PGA could have such a significantly beneficial effect demonstrates both the importance of the dimensions of the formed complexes and its cell-penetrating activity dynamics. We propose that the large P-R8-DOX/PGA complexes succeeded in temporarily inhibiting cell penetration during delivery, until such time as the complex had passively accumulated at the tumor site. However, further studies are required to clearly demonstrate that the improved mice survival rate was realized due to a specific de-shielding effect of R8 activity, rather than simply improved accumulation of the large P-R8-DOX/PGA complexes.

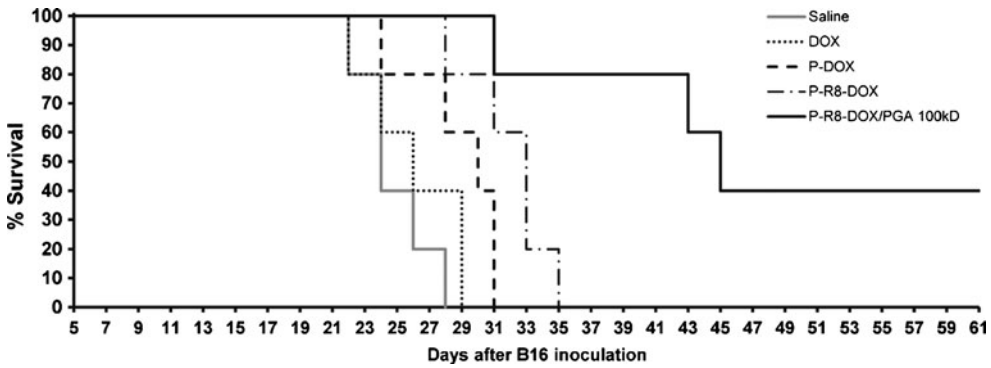

Fig. 8 *In vivo* experimental lung metastases and survival assay. 7 days after B16-F10 inoculation, mice were injected i.v. with P-DOX, P-R8-DOX, P-R8-DOX/PGA (100 kD) (1:3) at single dose of 15 mg/kg DOX equivalent, and with free DOX (6 mg/kg) or with saline, and then monitored for their survival (Kaplan-Meier method) for 60 days. $P < 0.005$ for P-R8-DOX/PGA compared to PBS, $P < 0.02$ compared to P-DOX, $P < 0.03$ compared to P-R8-DOX (by Student's t-test).

CONCLUSIONS

We have demonstrated that complexation of P-R8 with various polyanions renders P-R8 biologically inactive, and that its cell penetration and activity can be restored either passively over time, or actively following the addition of a stronger polycation. The resulting P-R8-DOX/PGA complexes substantially increased the anti-tumor activity of DOX, perhaps by increasing selectivity for the tumor site while controlling the rate of drug release from the complexes. If proven successful in additional *in vivo* assays, this novel approach for improved drug accumulation within solid tumors while controlling penetration into cells within the tumor micro-environment could offer a promising approach for the treatment of different kinds of solid tumors.

ACKNOWLEDGMENTS AND DISCLOSURES

This work was supported in part by grants from the Israel Science Foundation (ISF) (Grant No. 418/10 to AD) and the Israeli National Nanotechnology Initiative for a Focal Technology Area (FTA) on Nanomedicines for Personalized Theranostics (to AD). GA acknowledges support from the E.J. Safra center.

REFERENCES

1. Torchilin VP. Recent advances with liposomes as pharmaceutical carriers. Nat Rev Drug Discov. 2005;4:145–60.
2. Kopecek J, Kopeckova P. HPMA copolymers: origins, early developments, present, and future. Adv Drug Deliv Rev. 2010;62:122–49.
3. Egusquiaguirre SP, Igartua M, Hernandez RM, Pedraz JL. Nanoparticle delivery systems for cancer therapy: advances in clinical and preclinical research. Clin Transl Oncol. 2012;14:83–93.
4. Kataoka K, Harada A, Nagasaki Y. Block copolymer micelles for drug delivery: design, characterization and biological significance. Adv Drug Deliv Rev. 2001;47:113–31.
5. Lammers T, Hennink WE, Storm G. Tumour-targeted nanomedicines: principles and practice. Br J Cancer. 2008;99:392–7.
6. Khandare JJ, Minko T. Antibodies and peptides in cancer therapy. Crit Rev Ther Drug Carrier Syst. 2006;23:401–35.
7. Matsumura Y, Maeda H. A new concept for macromolecular therapeutics in cancer chemotherapy: mechanism of tumoritropic accumulation of proteins and the antitumor agent smancs. Cancer Res. 1986;46:6387–92.
8. Maeda H, Wu J, Sawa T, Matsumura Y, Hori K. Tumor vascular permeability and the EPR effect in macromolecular therapeutics: a review. J Control Release. 2000;65:271–84.
9. Netti PA, Berk DA, Swartz MA, Grodzinsky AJ, Jain RK. Role of extracellular matrix assembly in interstitial transport in solid tumors. Cancer Res. 2000;60:2497–503.
10. Brekken C, Bruland OS, de Lange Davies C. Interstitial fluid pressure in human osteosarcoma xenografts: significance of implantation site and the response to intratumoral injection of hyaluronidase. Anticancer Res. 2000;20:3503–12.
11. Lammers T, Kiessling F, Hennink WE, Storm G. Drug targeting to tumors: principles, pitfalls and (pre-) clinical progress. J Control Release. 2012;161:175–87.
12. Allen TM. Ligand-targeted therapeutics in anticancer therapy. Nat Rev Cancer. 2002;2:750–63.
13. David A. Carbohydrate-based biomedical copolymers for targeted delivery of anticancer drugs. Israel J Chem. 2010;50:204–19.
14. Karra N, Benita S. The ligand nanoparticle conjugation approach for targeted cancer therapy. Curr Drug Metab. 2012;13:22–41.
15. David A, Kopeckova P, Minko T, Rubinstein A, Kopecek J. Design of a multivalent galactoside ligand for selective targeting of HPMA copolymer-doxorubicin conjugates to human colon cancer cells. Eur J Cancer. 2004;40:148–57.
16. Shamay Y, Paulin D, Ashkenasy G, David A. E-selectin binding peptide-polymer-drug conjugates and their selective cytotoxicity against vascular endothelial cells. Biomaterials. 2009;30:6460–8.
17. Shamay Y, Paulin D, Ashkenasy G, David A. Multivalent display of quinic acid based ligands for targeting E-selectin expressing cells. J Med Chem. 2009;52:5906–15.
18. Adar L, Shamay Y, Journo G, David A. Pro-apoptotic peptide-polymer conjugates to induce mitochondrial-dependent cell death. Polym Adv Technol. 2011;22:199–208.
19. Kopansky E, Shamay Y, David A. Peptide-directed HPMA copolymer-doxorubicin conjugates as targeted therapeutics for colorectal cancer. J Drug Target. 2011;19:933–43.
20. Journo-Gershfeld G, Kapp D, Shamay S, Kopeček J, David A. Hyaluronan oligomers-HPMA copolymer conjugates for targeting paclitaxel to CD44-overexpressing ovarian Carcinoma. Pharm Res. 2012;29:1121–33.
21. Lindgren M, Hallbrink M, Prochiantz A, Langel U. Cell-penetrating peptides. Trends Pharmacol Sci. 2000;21:99–103.
22. Schwarze SR, Dowdy SF. In vivo protein transduction: intracellular delivery of biologically active proteins, compounds and DNA. Trends Pharmacol Sci. 2000;21:45–8.
23. Sethuraman VA, Bae YH. TAT peptide-based micelle system for potential active targeting of anti-cancer agents to acidic solid tumors. J Control Release. 2007;118:216–24.
24. Kale AA, Torchilin VP. Design, synthesis, and characterization of pH-sensitive PEG-PE conjugates for stimuli-sensitive pharmaceutical nanocarriers: the effect of substitutes at the hydrazone linkage on the ph stability of PEG-PE conjugates. Bioconjug Chem. 2007;18:363–70.
25. Jiang T, Olson ES, Nguyen QT, Roy M, Jennings PA, Tsien RY. Tumor imaging by means of proteolytic activation of cell-penetrating peptides. Proc Natl Acad Sci U S A. 2004;101:17867–72.
26. Olson ES, Aguilera TA, Jiang T, Ellies LG, Nguyen QT, Wong EH, *et al*. In vivo characterization of activatable cell penetrating peptides for targeting protease activity in cancer. Integr Biol (Camb). 2009;1:382–93.
27. Shamay Y, Adar L, Ashkenasy G, David A. Light induced drug delivery into cancer cells. Biomaterials. 2011;32:1377–86.
28. Rihova B, Bilej M, Vetvicka V, Ulbrich K, Strohalm J, Kopecek J, *et al*. Biocompatibility of N-(2-hydroxypropyl) methacrylamide copolymers containing adriamycin. Immunogenicity, and effect on haematopoietic stem cells in bone marrow in vivo and mouse splenocytes and human peripheral blood lymphocytes in vitro. Biomaterials. 1989;10:335–42.
29. Kopecek J, Bazilova H. Poly[N-(2-hydroxypropyl)methacrylamide] I. Radical polymerization and copolymerization. Eur Polym J. 1973;9:7–14.

30. Drobník J, Kopeček J, Labsk J, Rejmanová P, Exner J, Saudek V. Enzymatic cleavage of side chains of synthetic water-soluble polymers. Makromol Chem. 1976;177:2833–48.
31. Omelyanenko V, Kopeckova P, Gentry C, Kopecek J. Targetable HPMA copolymer-adriamycin conjugates. Recognition, internalization, and subcellular fate. J Control Release. 1998;53:25–37.
32. Etrych T, Jelinkova M, Rihova B, Ulbrich K. New HPMA copolymers containing doxorubicin bound via pH-sensitive linkage: synthesis and preliminary in vitro and in vivo biological properties. J Control Release. 2001;73:89–102.
33. Seymour LW, Ulbrich K, Steyger PS, Brereton M, Subr V, Strohalm J, *et al*. Tumour tropism and anti-cancer efficacy of polymer-based doxorubicin prodrugs in the treatment of subcutaneous murine B16F10 melanoma. Br J Cancer. 1994;70:636–41.
34. Kwon YM, Li Y, Naik S, Liang JF, Huang Y, Park YJ, *et al*. The ATTEMPTS delivery systems for macromolecular drugs. Expert Opin Drug Deliv. 2008;5:1255–66.